Characterisation of ferroelectric poly(vinylidene fluoride–trifluoroethylene) film prepared by Langmuir-Blodgett deposition

Woo Young Kim[1,†], Dong-Seok Song[2,†], Gwang-Jae Jeon[3], In Ku Kang[3], Hyun Bin Shim[3], Do-Kyung Kim[2], Hee Chul Lee[3], Hongsik Park[2], Shin-Won Kang[2], Jin-Hyuk Bae[2]

[1]*Department of Mechanical Engineering, Korea Advanced Institute of Science and Technology (KAIST), Daejeon 706-091, Republic of Korea*
[2]*School of Electronics Engineering, Kyungpook National University, Daegu 702-701, Republic of Korea*
[3]*Department of Electrical Engineering, Korea Advanced Institute of Science and Technology (KAIST), Daejeon 706-091, Republic of Korea*
[†]*These authors equally contributed to this work.*
E-mail: jhbae@ee.knu.ac.kr

Published in Micro & Nano Letters; Received on 28th January 2015; Accepted on 18th May 2015

Ferroelectric polymer is a flexible memory material that is insensitive to environmental variations and lends itself to research in emerging optoelectronic applications. Using Langmuir-Blodgett (LB) deposition technology, the thickness of a ferroelectric film can be controlled in the nanometre range, offering a pathway to molecular electronics. In this reported work, ultrathin ferroelectric polymer films were fabricated through LB deposition technology and characterised by observing the surface morphology, crystallinity and polarisation–voltage relationships. Unlike previously reported ferroelectric LB films, this work has shown a maximum remanent polarisation (P_R) of 6 μC/cm^2 at 35 nm, which is compatible with the thick film prepared by the spin-coating method. In addition, the polarisation stability in terms of depolarisation was investigated, which showed that the engineering of the interface between the ferroelectric LB film and the substrate is an important, deterministic factor for reliable memory applications with high signal-to-noise ratios.

1. Introduction: Ferroelectric materials exhibit spontaneous polarisation even without an external electric field, which enables them to be switched. By assigning each polarisation state to a logic state (0 or 1), digital data can be stored in a memory medium, such as a ferroelectric material. Currently, inorganic ferroelectric materials, such as lead zirconium titanate (PZT) and strontium bismuth tantalate are widely utilised as memory media in such devices as portable appliances and identification cards [1]. Recently, it was also reported that a PZT thin film could be made flexible by being transferred onto a flexible substrate, which presents possibilities for high-performance flexible non-volatile memory in wearable systems [2]. However, further emerging applications and technologies are elusive in large-area systems, transparent devices and vacuum-free processes because of the limitations of inorganic materials. Moreover, the lead in PZT has been the subject of controversy because of its toxicity [3]. In terms of materials, ferroelectric polymer can provide a solution to this conundrum. In particular, the polymers based on poly(vinylidene fluoride) have received considerable attention for their superior ferroelectricity and the ease with which they can be incorporated into devices, in that the remanent polarisation is about 10 μC/cm^2, retention time is nearly infinite and the material can be made ferroelectric by simple annealing at a temperature above the Curie temperature [4]. Transparency in visible light and mechanical flexibility are bonus features for emerging applications [5]. Compared with inorganic ferroelectric materials, there is a complicated problem we must deal with for this material: the coercive field. Ferroelectric polymer has a coercive field of a few MV/cm, whereas PZT has one of about 10 kV/cm. To bypass such high-voltage operation, the thickness of the ferroelectric polymer should be reduced. Although spin-coating with a diluted solution at a fast spin speed for quite a long time results in an ultrathin film, this is impractical according to previous reports, resulting in nanometre-scale holes that cause electrical short circuits [6]. Instead, the Langmuir-Blodgett (LB) deposition method is offering an attractive way to achieve nanometre-scale thickness. Through the LB deposition method, as shown in Fig. 1*a*, it was possible to transfer a ferroelectric polymer monolayer from the interface between air and water, and the repetition of LB deposition can be used to control the film thickness layer by layer; this approach can lead to molecular electronics applications [7]. In the work reported in this Letter, a ferroelectric film was prepared by LB deposition to control the film thickness, which was characterised by observation of the surface morphology, crystallinity and polarisation–voltage relationships. From this characterisation, it was concluded that interface engineering is critical in terms of polarisation stability for reliability.

2. Experimental details: A pellet type of poly(vinylidene fluoride–trifluoroethylene), P(VDF–TrFE), was purchased from MSI Sensors Inc.; the molecular ratio of PVDF to PTrFE was 75:25.A measure of 5×10^{-4} g of P(VDF–TrFE) was dissolved in 1 ml of dimethyl sulphoxide (DMSO) (solution concentration =0.05 wt%) under 12 h of stirring, which was then filtered to remove the P(VDF–TrFE) residue. The solution was dropped into deionised water in a trough made of Teflon using a micropipette. Using a

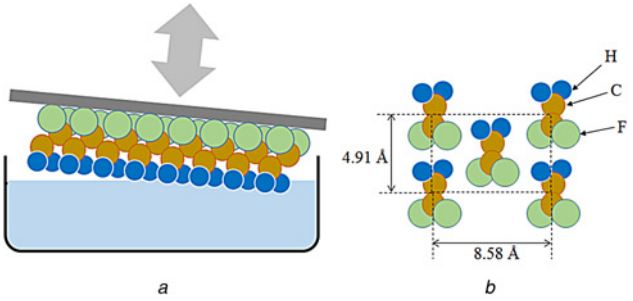

Figure 1 *LB deposition*
a Schematic of the horizontal transfer method
b Depiction of the lattice constant in *β*-phase P(VDF–TrFE) film

doi: 10.1049/mnl.2015.0038

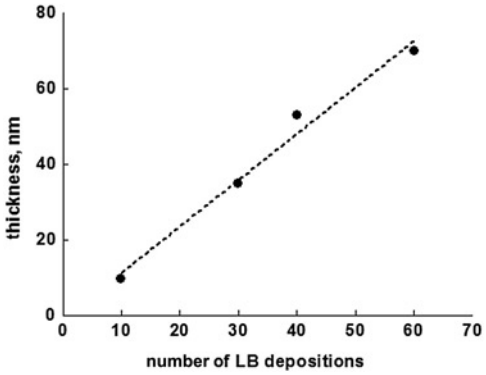

Figure 2 *Relationship between the number of LB depositions and film thickness*

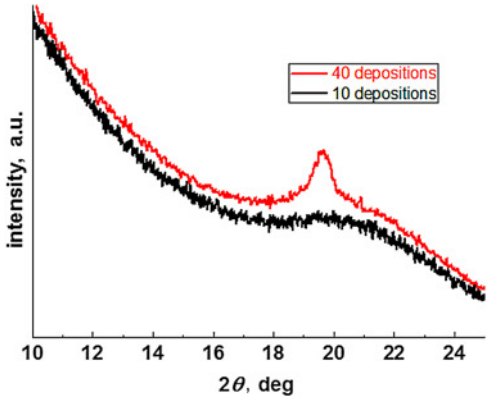

Figure 4 *XRD measurements for 10 LB depositions and 40 LB depositions*

homemade automated controlled barrier, the P(VDF–TrFE) molecules on the water surface were compressed. Next, the molecular film was transferred by the horizontal transfer method, as depicted in Fig. 1. The surface tension for the transfer was maintained at 5×10^{-5} N/cm, and the substrate was contacted with an angle of 10° at the water surface. The transfer speed was 1 mm/s or less because the uniformity of the LB film is very sensitive to the transfer speed [8]. The thickness of the LB film was controlled by repeated transfers, and it was measured using an α-step profiler (Dektak 6 M, Veeco Instruments Inc.). The substrate was glass with indium–tin-oxide (ITO) deposited on it. The surface morphology of the LB film was measured with an atomic force microscope (AFM, XE-100, Park Systems Corp.). X-ray diffraction measurements were performed with an X-ray diffractometer (D/MAX-2500, Rigaku). To measure the electrical properties of the LB film, the top electrode of Au was thermally evaporated through a metallic shadow mask in a high-vacuum chamber (1.2×10^{-6} Torr). The Au evaporation rate was maintained below 0.3 Å/s. The electrode was circular in shape, with a diameter of 180 µm and an area of 2.54×10^{-4} cm^2. Polarisation–voltage (P–V) hysteresis loops were measured in the virtual ground mode of a ferroelectric measurement system, RT-66A (Radiant Technologies Inc.), which is a Sawyer-Tower circuit modified to eliminate the artefacts from parasitic capacitance.

3. Results and discussion: Fig. 2 shows the relationship between the number of LB depositions and the thickness of the LB film; the plot indicates a linear proportionality between these parameters. The slope of the linear fit is 1.2 ± 0.11 nm. The lattice constant of the β-phase of P(VDF–TrFE) vertical to the substrate is 4.91 Å, as shown in Fig. 1*b*; therefore the film thickness increases at a rate of nearly two monolayers per LB deposition, as previously stated in the literature [8].

Fig. 3 shows the surface morphologies of the P(VDF–TrFE) LB film prepared by 10 LB depositions and 40 LB depositions. For 10 LB depositions, its root mean square (RMS) roughness was about 1.15 nm, which corresponds to the RMS roughness values for the spin-coated film with a similar thickness. The RMS roughness value increases to 7.76 nm for the case of 40 LB depositions, which is a much larger value than that of the spin-coated film. It has been reported that crystallinity also increases as film thickness increases [9], which may be the reason for such a large RMS value of the LB film prepared by 40 LB depositions. Another explanation for the increase in RMS roughness value may be the formation of the nanomesa structure [10].

Fig. 4 shows the XRD measurement results for the two P(VDF–TrFE) LB films. For 10 LB depositions, the peak corresponding to the β-phase in the P(VDF–TrFE) film was not observed at $2\theta = 19.8°$. In contrast, the film prepared by 40 LB depositions shows a strong peak in the β-phase. From these results, it is concluded that an LB film as thin as 10 nm forms an amorphous phase, which may originate from a lattice mismatch between the electrode and P(VDF–TrFE) [11]. This layer can act as an interfacial dead layer when a metal/LB film/metal structure is formed to create a capacitor or a metal/LB film/semiconductor structure is formed to create a transistor. In addition, the crystal size in the LB film prepared by 40 LB depositions was calculated to be 13.3 nm using

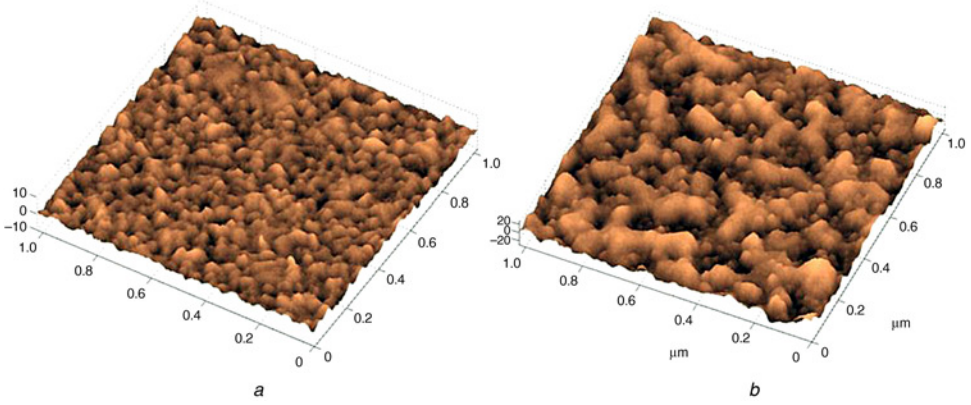

Figure 3 *Surface morphology of LB films for 10 LB and 40 LB depositions in an area of 1 µm × 1 µm*
a 10 LB depositions
b 40 LB depositions

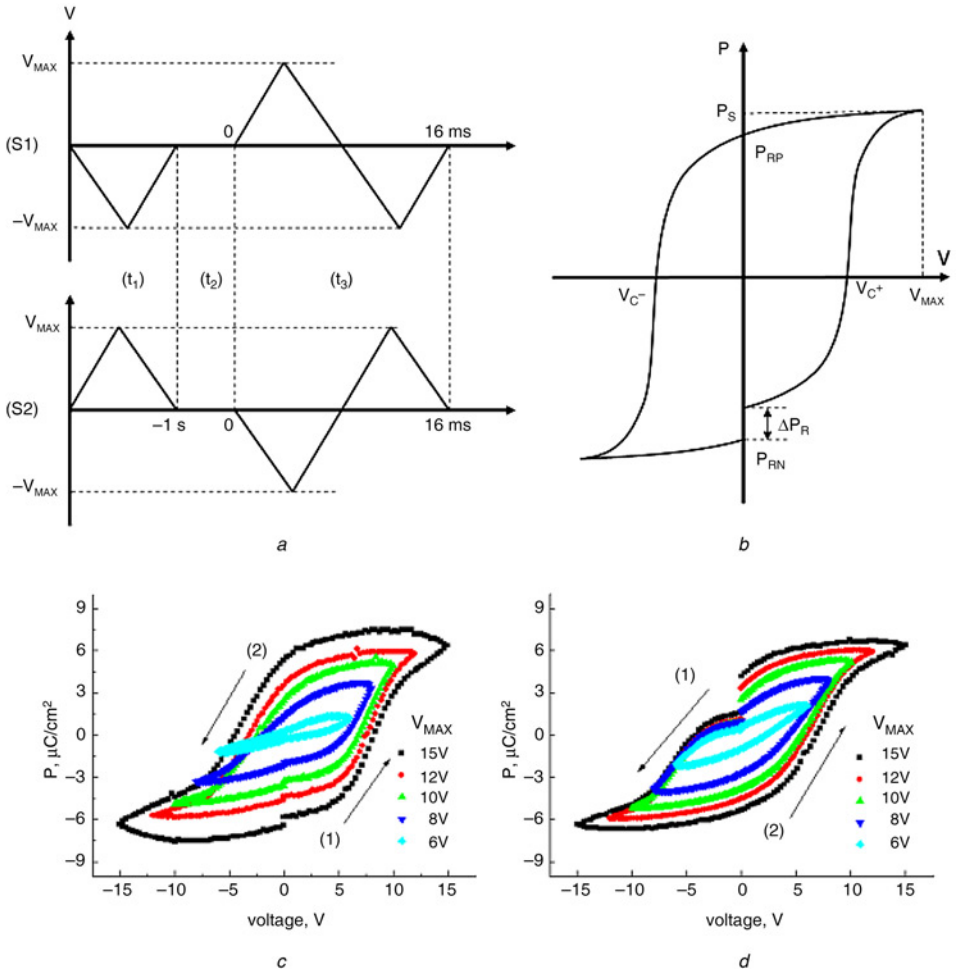

Figure 5 *P–V relationships*
a Schematic of the two signal profiles (S1) and (S2)
(*t*1) is the time at which the polarisation is initialised, (*t*2) is a delay time of 1 s to allow for polarisation stabilisation and (*t*3) is the hysteresis loop measurements (which have a duration of 16 ms)
b Depiction of the notation used for parameters for saturation polarisation (P_S), positive and negative remanent polarisations (P_{RP}, P_{RN}), positive and negative coercive voltages (V_C^+, V_C^-), and depolarisation (ΔP_R) [12]
c *P–V* relationship measured with the (S1) profile
d *P–V* relationship measured with (S2)
Labels '(1)' and '(2)' in Figs. 5*c* and *d* represent the sweep directions of voltage

the Scherrer equation as follows:

$$\tau = \frac{K\lambda}{B\cos\theta} \tag{1}$$

where τ is the mean size of the crystals, λ the X-ray wavelength, B the full width at half maximum and θ is the Bragg angle.

To characterise the electrical performances, *P–V* relationships were measured for a 35 nm-thick LB film (30 LB depositions) capacitor using the two voltage signal profiles (S1) and (S2) depicted in Fig. 5*a*. The differences between the two signals were the voltage sweep direction and the order of the signals. For the case of (S1), a negative pulse was applied to initialise the polarisation to a negative remanent polarisation (P_{RN}) before we began to measure the hysteresis loop, whereas a positive pulse was applied for initialisation of the positive remanent polarisation (P_{RP}) in the case of (S2). Immediately after initialisation, a delay time of 1 s elapsed before the hysteresis loop was measured. Observation of the polarisation after this delay time provides an opportunity to identify the time-dependent stability of each P_R value [12]. Related notations and symbols are expressed in Fig. 5*b*.

Figs. 5*c* and *d* illustrate the *P–V* relationships measured with the signal profiles of (S1) and (S2), respectively, and the related parameters are plotted in Fig. 6. What is promising is that the P_R values have a maximum of 6 μC/cm^2, which is compatible with the P_R values in spin-coated thick films [13]. Previous PVDF-based LB films showed a strong thickness dependence of the P_R values, especially below a thickness of 50 nm [14], which means that the shrinkage of the thickness can serve as an advantage for low-voltage operation, but memory devices with high signal-to-noise ratios (SNRs) cannot be achieved. Here, the high P_R values are thought to be achieved by the use of an inert electrode (such as one made of Au) and a slow evaporation rate [15].

The second consideration is that the hysteresis loop is continuous or discontinuous at $V = 0$. For the case where P_{RN} was stored by initialisation, the ΔP_{RN} values, defined as P_{RN} (16 ms)–P_{RN} (0), are nearly zero, while the ΔP_{RP} values, defined as P_{RP} (16 ms)–P_{RP} (0), are relatively large for storage of P_{RP}. In other words, logic state '1' (corresponding to P_{RN}) is stored longer than logic state '0' (for P_{RP}) because the digital information about the '0' value relaxed even within 1 s after it was written. This polarisation relaxation can be explained by the depolarisation field, described by the following equation [16]:

doi: 10.1049/mnl.2015.0038

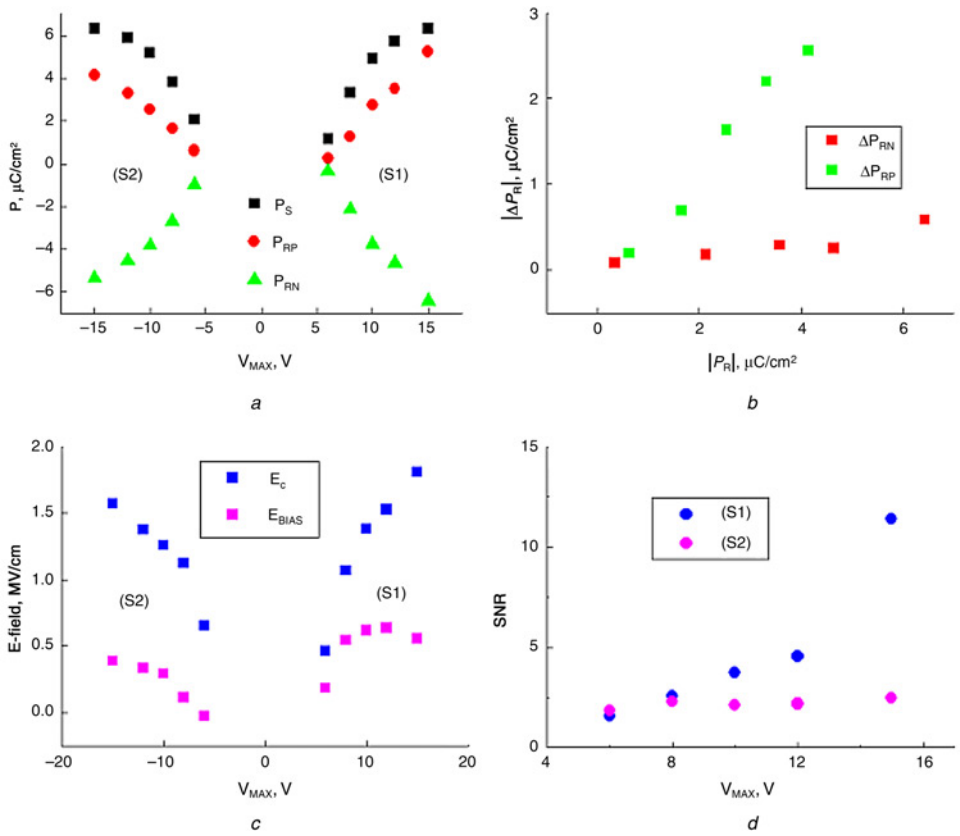

Figure 6 *Parameters extracted from P–V measurements*
a Saturation polarisation (P_S) and remanent polarisations (P_{RP} and P_{RN}) against V_{MAX}
b Depolarisations (ΔP_{RP} and ΔP_{RN}) against the magnitude of the remanent polarisation ($|P_R|$)
c Coercive field (E_C) and internal bias field (E_{BIAS}) for (S1) and (S2)
d SNR for signal profiles S1 and S2

$$E_{dp} = P\left[\varepsilon_F\left(1+\frac{C_i}{C_F}\right)\right]^{-1} \tag{2}$$

where E_{dp} is the depolarisation field, P the polarisation, ε_F the dielectric constant of the ferroelectric film, C_i the capacitance of the interfacial dead layer and C_F is the capacitance of the ferroelectric film.

The quantity of depolarisation increases as E_{dp} increases, which is directly proportional to the polarisation (P) value in (2). From the relationship between $|P_R|$ and ΔP_R in Fig. 6*b*, it seems that the depolarisation field is a factor that has influence over the reduction of P_{RP}. The E_{dp} value can be maximised when an interfacial dead layer exists between the electrode and the ferroelectric layer and contributes to C_i in (2). From the XRD measurements in Fig. 4, the interfacial dead layer is thought to be the reason for the existence of E_{dp}. Another factor in the depolarisation may be the internal bias field, which causes the P–V hysteresis loop to be shifted along the x-axis. For the sake of further analysis, the coercive field ($E_C = (V_C^+ + V_C^-)/2d$) and the internal bias field ($E_{BIAS} = (V_C^+ - V_C^-)/2d$) values with a film thickness (d) of 35 nm are calculated and shown in Fig. 6*c*. The E_{BIAS} values are nearly 30–50% of E_C; therefore, the built-in potential could be generated and affect the depolarisation.

The degradation of the P_R values reduces the SNR in data decoding. When the architecture of the destructive readout is adopted in the ferroelectric memory, the SNR value is defined as the ratio of the switched polarisation ($P_S + P_R$) to the non-switched polarisation ($P_S - P_R$):

$$\mathrm{SNR}_{S1} = \frac{P_S + (P_{RN} - \Delta P_R)}{P_S - P_{RP}} \tag{3.1}$$

$$\mathrm{SNR}_{S2} = \frac{P_S + P_{RN}}{P_S - (P_{RP} - \Delta P_R)} \tag{3.2}$$

Here, SNR_{S1} and SNR_{S2} are equations for Figs. 5*c* and *d*, respectively. The depolarisation ΔP_R reduces the signal component in the numerator for SNR_{S1}, whereas it increases the noise component in the denominator for SNR_{S2}. Fig. 6*d* shows that the SNR values are seriously affected by the shape of the hysteresis loop; therefore, depolarisation needs to be reduced by process optimisation, such as the insertion of stress-relaxed conducting buffer layers between the electrode and the ferroelectric film.

4. Conclusion: In this reported work, the thickness of the P(VDF–TrFE) was reliably controlled on the nanometre scale by using LB deposition. From AFM and XRD measurements, it was found that the crystallinity could be increased as the thickness increased. For the case of 40 LB depositions, the crystal size was calculated to be 13 nm. The electrical performance revealed that the time-dependent polarisation stability was quantified in terms of depolarisation, which is a critical parameter for application to non-volatile memory devices. By calculation of the depolarisation and internal bias field, it is concluded that the engineering of the interface between an ultrathin ferroelectric film and the substrate is one of the dominant issues that must be addressed for further investigation of emerging optoelectronic applications.

5. Acknowledgments: This work was supported by a Preparatory Project (N10110074) at the Korea Advanced Institute of Science and Technology (KAIST). This work was also supported by the Basic Science Research Program through the National Research Foundation of Korea (NRF) funded by the Ministry of Education (2013R1A1A4A01009807) and by the Korea government (MSIP) (no. 2008-0062617).

6 References

[1] http://www.fujitsu.com/downloads/MICRO/fme/fram/fram-guide-book.pdf
[2] Lee W., Kahya O., Toh C.T., Ozyilmaz B., Ahn J.-H.: 'Flexible graphene–PZT ferroelectric nonvolatile memory', *Nanotechnology*, 2013, **24**, pp. 475202-1–475202-6
[3] Sluka T., Tagantsev A.K., Damjanovic D., Gureev M., Setter N.: 'Enhanced electromechanical response of ferroelectrics due to charged domain walls', *Nat. Commun.*, 2012, **3**, doi: 10.1038/ncomms1751
[4] Naber R.C.G., Asadi K., Blom P.W.M., Leeuw D.M., Boer B.: 'Organic nonvolatile memory devices based on ferroelectricity', *Adv. Mater.*, 2010, **22**, pp. 933–945
[5] Ni G.-X., Zheng Y., Bae S., *ET AL.*: 'Graphene-ferroelectric hybrid structure for flexible transparent electrodes', *ACS Nano*, 2012, **6**, pp. 3935–3942
[6] Lee H.J., Kim Y.-J., Lee E., Yao K., Jo J.Y.: 'Topography engineering of ferroelectric crystalline copolymer film', *Org. Electron.*, 2014, **15**, pp. 751–757
[7] Jiang Y., Ye Y., Yu J., Yang Y., Xu J., Wu Z.: 'A study on ferroelectric PVDF ultrathin films prepared by LB technique', *Integr. Ferroelectr.*, 2007, **88**, pp. 21–26
[8] Ducharme S., Reece T.J., Othon C.M., Rannow R.K.: 'Ferroelectric polymer Langmuir-Blodgett films for nonvolatile memory applications', *IEEE Trans. Device Mater. Rel.*, 2005, **5**, pp. 720–735
[9] Zhang Q.M., Xu H., Fang F., Cheng Z.-Y., Xia F., You H.: 'Critical thickness of crystallization and discontinuous change in ferroelectric behavior with thickness in ferroelectric polymer thin films', *J. Appl. Phys.*, 2001, **89**, pp. 2613–2616
[10] Bai M., Poulsen M., Ducharme S.: 'Effects of annealing conditions on ferroelectric nanomesa self-assembly', *J. Phys.*, 2006, **18**, pp. 7383–7392
[11] Zhang Y., Zhong X.L., Vopson M., Wang J.B., Zhou Y.C.: 'Thermally activated polarization dynamics under the effects of lattice mismatch strain and external stress in ferroelectric film', *J. Appl. Phys.*, 2012, **112**, pp. 014112-1–012112-7
[12] Inoue N., Hayashi Y.: 'Effect of imprint on operation and reliability of ferroelectric random access memory (FeRAM)', *IEEE Trans. Electron Devices*, 2001, **48**, pp. 2266–2272
[13] Kim W.Y., Ka D.Y., Kim D.S., *ET AL.*: 'Internal bias field in ferroelectric polymer thin film for nonvolatile memory applications', *IEEE Electron Device Lett.*, 2010, **31**, pp. 482–484
[14] Zhu H., Yamamoto S., Matsui J., Miyashita T., Mitshushi M.: 'Ferroelectricity of poly(vinylidene fluoride) homopolymer Langmuir-Blodgett nanofilms', *J. Mater. Chem. C*, 2014, **2**, pp. 6727–6731
[15] Naber R.C.G., Blom P.W.M., Leeuw D.M.: 'Comment on "Extrinsic versus intrinsic ferroelectric switching: experimental investigations using ultra-thin PVDF Langmuir-Blodgett films" ', *J. Phys. D, Appl. Phys.*, 2006, **39**, pp. 1984–1986
[16] Ma T.P., Han J.-P.: 'Why is nonvolatile ferroelectric memory field-effect transistor still elusive?', *IEEE Elecctron Device Lett.*, 2002, **23**, pp. 386–388

doi: 10.1049/mnl.2015.0038